Observational Study

Medicine®

OPEN

Diagnostic value of diffusion-weighted magnetic resonance imaging for local and skull base recurrence of nasopharyngeal carcinoma after radiotherapy

Chen Wang, MD, Lidong Liu, MD, Shaolv Lai, MD*, Danke Su, MD, Younan Liu, MD, Guanqiao Jin, MD, Xuna Zhu, MD, Ningbin Luo, MD

Abstract

Tumor recurrence is a major cause of nasopharyngeal carcinoma (NPC) treatment failure. Diffusion-weighted imaging (DWI) is used for a variety of cancers, but few data are available for NPC.

The aim of the study was to investigate the DWI features of recurrent NPC after radiotherapy and apparent diffusion coefficient (ADC) thresholds for the diagnosis of recurrent NPC.

This was a retrospective study of 160 patients with NPC treated by radiotherapy at the Cancer Hospital affiliated to Guangxi Medical University from May 2012 to March 2015. The patients were divided into the local recurrence (n = 39), fibrosis (n = 51), clivus recurrence (n = 22), and clivus nonrecurrence (n = 48) groups. The patients underwent magnetic resonance imaging (MRI), enhanced MRI, and DWI. Receiver operating characteristics curves were used to determine sensitivity, specificity, and negative predictive values.

ADC values were significantly different between the recurrence and fibrosis groups ($P < .0001$). Using ADC threshold values of 0.887×10^{-3} mm^2/s for local recurrence, the area under the curve (AUC) of DWI was 0.967 (87.2% sensitivity and 94.1% specificity), compared with 0.732 for routine MRI (71.8% sensitivity and 74.5% specificity) ($P < .001$). Using ADC threshold values of 1.018×10^{-3} mm^2/s for the diagnosis of clivus recurrent NPC, the AUC of DWI was 0.984 (95.5% sensitivity and 91.7% specificity) compared with 0.558 for routine MRI (63.6% sensitivity and 47.9% specificity) ($P < .001$).

DWI has a higher diagnostic value for recurrent NPC than MRI. DWI can increase the diagnosis sensitivity and specificity of locally recurrent NPC.

Abbreviations: ADC = apparent diffusion coefficient, AUC = area under the curve, CT = computed tomography, DWI = diffusion-weighted imaging, MRI = magnetic resonance imaging, NPC = nasopharyngeal carcinoma, PET = positron emission tomography, ROC = receiver operating characteristics, ROI = regions of interest, TSE = T1-weighted turbo spin-echo.

Keywords: diffusion-weighted imaging, fibrosis, magnetic resonance imaging, nasopharyngeal carcinoma, recurrence

1. Introduction

Nasopharyngeal carcinoma (NPC) is a common cancer type in Southern Asia, with an incidence accounting for approximately 40% of the world's new cases, according to the World Health Organization's GLOBOCAN 2012 data.[1,2] NPC is very sensitive to radiotherapy and/or adjuvant chemotherapy. After standard treatments, the recurrence rates of stages T1-T2, T3, and T4 NPC are 1%, 6%, and 17%, respectively.[3] The 5-year survival rate of patients with skull base involvement is only 26.9%, and the 5-year survival rate is decreased to 7.7% if the patients are with involvement of both the anterior and posterior groups of cranial nerves.[4,5]

Tumor recurrence is still one of the most important causes of treatment failure for NPC patients. After radiotherapy, most patients with NPC still have a local lump, which has to be differentiated from residual tumor, fibrosis, and recurrence. Approximately 42.9% of the recurrent NPCs are at the clivus of the skull base.[6] Early identification of recurrent NPCs is important to reduce mortality.

For the diagnosis of NPC recurrence, the most direct method is nasopharyngoscopic needle biopsy,[6] but growth and invasion patterns of the recurrent NPC, inflammation after radiotherapy, and scars can make it difficult to obtain appropriate biopsies from the nasopharynx.[6] Even in the case that the conditions for nasopharyngoscopic needle biopsy are met, misdiagnosis can still occur due to sampling bias. In addition, the structures of the skull base are very deep and the anatomical structures are very complex. Therefore, the diagnosis of skull base recurrence of NPC mainly depends on long-term imaging follow-up.[6] The application of ^{18}F-FDG and positron emission tomography

Editor: Heye Zhang.

The authors CW and LDL contributed equally to this work.

The authors have no conflicts of interest to disclose.

Department of Radiology, Affiliated Cancer Hospital of Guangxi Medical University, Nanning, Guangxi, P.R. China.

* Correspondence: Shaolv Lai, Department of Radiology, Affiliated Cancer Hospital of Guangxi Medical University, Nanning, Guangxi, 530021, P.R. China (e-mail: lsl1688@139.com).

Medicine (2018) 97:34(e11929)

Received: 3 November 2017 / Accepted: 21 July 2018

http://dx.doi.org/10.1097/MD.0000000000011929

(PET)/computed tomography (CT) has great importance in the diagnosis and localization of NPC recurrence, differential diagnosis of residual lesions, assessment of the changes after radiotherapy, clinical staging of the recurrent NPC, selecting treatment strategies, and assessment of treatment effectiveness.[7,8] Nevertheless, such methods also have several limitations such as relatively high medical expenses, high false positive and false negative rates, availability, and radiations.[7,8] Conventional CT and/or magnetic resonance imaging (MRI) also have significant limitations for the early identification of recurrent lesions from nasopharyngeal fibrosis post radiotherapy in the area of the nasopharynx and skull base.[9] Therefore, an accurate noninvasive method to detect recurrence during follow-up after NPC is needed.

Diffusion-weighted imaging (DWI) is a functional imaging technique that can provide information about the tissues biophysical properties, based on the Brownian motion of water molecules in biological tissues. The apparent diffusion coefficient (ADC) can be measured, which is sensitive to certain parameters such as cell organization, cell density, microstructure, and microcirculation.[10,11] At present, DWI has been used in abdominal areas, vertebral bodies, limbs, joints, breasts, and other parts of the body,[10,12–16] but few study reported its use in recurrent NPC.

Therefore, the purpose of this study was to investigate the DWI features of recurrent NPC after radiotherapy, the changes of the nasopharynx and skull base after radiotherapy, and ADC thresholds for the diagnosis of recurrent NPC.

2. Materials and methods

2.1. Study design

This was a retrospective study of 1175 consecutive patients with NPC treated with radiotherapy at the Cancer Hospital affiliated to Guangxi Medical University from May 2012 to March 2015. All these patients were treated with radical radiotherapy at least 6 months before. All patients with NPC treated with radiotherapy and without chemotherapy were included. The exclusion criteria were loss to follow-up; missing data; metal artifacts affecting MRI; or they did not undergo any clinical management despite suspicion of NPC recurrence.

This study was approved by the ethics committee of Guangxi Medical University affiliated cancer hospital. An informed consent was obtained from each patient.

2.2. Grouping of the patients

The patients were categorized into 4 groups: clivus recurrence group, local recurrence group, fibrotic group, and clivus nonrecurrence group. The patients were categorized into the local recurrence group (patients with local NPC recurrence after radiotherapy) if they met one of the following criteria: the primary tumor disappeared after radiotherapy, whereas MRI re-examination at ≥6 months later showed that the lesion at the nasopharynx had reappeared or increased and pathological examinations of the biopsies confirmed tumor recurrence; the primary tumor disappeared after radiotherapy; MRI re-examination at ≥6 months later showed that the lesion at the nasopharynx had reappeared or increased, but was not confirmed by pathological examinations; nevertheless, re-treatment with radiotherapy resulted in tumor regression (DWI scanning was conducted before re-treatment).

The patients were categorized into the fibrosis group if the pathological examinations of the needle biopsies at ≥12 months after radiotherapy confirmed fibrosis, or if MRI re-examinations showed one of the following criteria: the morphology of the nasopharynx was stable and not changed and the patients were highly suspected to be with NPC recurrence, but follow-up imaging after radiotherapy did not show the suspicious lesion.

The patients were categorized into the clivus recurrence group if they met the following criteria: MRI before treatment showed the NPC involvement of the clivus of the skull base, whereas MRI after the initial treatments showed that the lesions at the nasopharynx and skull base regressed or disappeared; the MRI at ≥6 months after radiotherapy showed that the lesions at the nasopharynx and skull base had reappeared or increased, with the features of signals and enhancement that were similar to the pre-treatment MRI; and biopsies of the nasopharynx confirmed NPC recurrence.

The patients were categorized into the clivus nonrecurrence group if they met the following criteria: pathological examinations confirmed that the patients were with NPC, pre-treatment MRI showed the NPC involvement of the clivus, and MRI after treatments showed that the lesions at the nasopharynx and skull base had regressed or disappeared and multiple MRI re-examinations at ≥6 months after treatments showed no new lesion at the nasopharynx or clivus, and the clinical and laboratory examinations showed no evidence of recurrence.

2.3. Imaging protocol

All patients were conventionally scanned with T1-weighted imaging (axial, coronal, and sagittal), fat suppressed T2-weighted imaging coronal, and axial DWI using a 1.5 T clinical MRI system (Magnetom Avanto, Siemens, Erlangen, Germany) using a standard combined head and neck coil. The scanned region extended from the upper edge of the suprasellar cistern to the lower edge of the third cervical vertebrae. Additional scans were conducted if necessary. T1-weighted turbo spin-echo (TSE) images in the axial, coronal, and sagittal planes (repetition time [TR]/echo time [TE] = 957 ms/19 ms; field of view (FOV) = 24 × 24 cm; slice thickness = 5.0 cm; slice gap = 1.0 mm; frequency matrix = 256 × 256), T2-weighted fat-suppressed turbo spin-echo (TSE) MRI in the axial plane (TR/TE = 6760 ms/91 ms; FOV = 24 × 24 cm; slice thickness = 5.0 mm; slice gap = 1.0 mm; frequency matrix = 384 × 384), and a spin-echo-echo-planar DWI sequence (TR/TE = 3400 ms/100 ms; slice thickness = 5 mm; slice gap = 1 mm; frequency matrix = 192 × 192, FOV = 23 × 23 cm; b values = 0 and 800 s/mm^2; and 3 signal averages) were obtained before contrast injection. After the intravenous administration of gadopentetate dimeglumine (0.2 mL/kg of body weight; Magnevist, Schering, Berlin, Germany), axial, sagittal, and coronal T1-weighted fat-suppressed spin-echo sequences were performed sequentially using the same parameters as before the injection. Then, 5-mm thick sections were obtained with a 1-mm interslice gap for the axial plane, resulting in a matrix size of 256 × 256.

2.4. MRI analysis

Imaging diagnoses were reviewed by 3 senior radiologists using matched MB17 workstations provided by Siemens. All 3 radiologists were experienced in diagnosing NPC for >10 years and independently reviewed the conventional MRI and MR DWI images. None of these 3 radiologists were aware of the final diagnosis and grouping of the patients. The diagnoses agreed by at least 2 radiologists were considered as the diagnoses of the conventional MRI and MR DWI.

For DWI analysis, the locations of the lesions were analyzed on DWI and ADC maps combined with conventional MRI. The layer with the largest lesion area was selected and the areas of liquefactive necrosis were avoided when ADC values were measured in 3 intralesion regions of interest (ROIs). The ROIs were no less than half of the maximum area of the target lesions. The average of the measurements was used for analysis.

2.5. Determination of local residual lesion and local recurrence of NPC after radiotherapy

The assessment criteria were established according to the literature in combination with the clinical experience of the radiologists.

(1) Locally residual NPC: within 6 months after radiotherapy, MRI was performed in followed patients and identified unsatisfactory regression of the NPC, NPC progression, or unchanged NPC. Results were confirmed by histopathology.
(2) Locally nonresidual tumor in the nasopharynx: shrunk or disappeared NP was identified by monthly nasopharyngeal MRI conducted after radiotherapy.
(3) Locally recurrent NPC: newly emerged tumors or damaged adjacent tissues in the nasopharynx were observed by MRI during follow-up >6 months after radiotherapy. The MRI findings were concurrent with aggravation of the clinical symptoms of the nasopharynx, and the results were confirmed by histopathology.
(4) Locally nonrecurrent NPC: unchanged morphology, tumor shrinkage, or tumor disappearance was observed in the nasopharynx by clinical or MRI follow-up for more than a year, with no newly emerging surrounding structural damage or signs of infiltration.

2.6. Statistical analysis

Continuous data were tested for normal distribution using the Kolmogorov-Smirnov test. Normally distributed continuous data were presented as mean ± standard divisions and analyzed using analysis of variance with the Tukey post hoc test. Categorical data were presented as frequencies and analyzed using the Fisher exact test. MedCalc 12.7 (MedCalc, Ostend, West Flanders, Belgium) was used to compare the diagnoses of the patients based on conventional MRI and MR DWI images, to obtain the receiver operating characteristics (ROC) curve, and to calculate the sensitivity and specificity of conventional MRI and MR DWI images for locally recurrent NPC. The areas under the conventional MRI and MR DWI ROC curves were compared with the z test. SPSS 22.0 (IBM, Armonk, NY) was used for statistical analysis. Two-sided P values $<.05$ were considered statistically significant.

3. Results

3.1. Characteristics of the patients

Among the 1175 eligible patients, 833 patients were excluded for being lost to follow-up, 93 for missing data, 68 for serious metal artifacts affecting MRI, and 21 because they did not receive any management despite suspicion of NPC recurrence. Finally, 160 patients were included in this study. They were 48 (21–82) years old and 81.2% were men. The median disease duration of these patients was 7 years (ranging from 1 to 13 yr) (Table 1).

Table 1

Characteristics of the patients.

Characteristics	Values
Age, yr	
Median	48
Range	21–82
Group, n (%)	
Local recurrent group	39 (24.4)
Fibrotic group	51 (31.8)
Clivus recurrent group	22 (13.8)
Clivus nonrecurrent group	48 (30.0)
Sex, n (%)	
Male	130 (81.2)
Female	30 (18.8)
T category, n (%)*	
T1	10 (16.39)
T2	11 (18.03)
T3	16 (26.22)
T4	24 (39.34)

* According to the 7th UICC/AJCC staging system.

3.2. Pathological and follow-up results

Among the 160 patients, 39 were in the local recurrent group (including 32 men and 7 women); their median age was 49 years (ranging from 26 to 82 yr). Thirty patients were confirmed with nonkeratinizing carcinoma by pathological examinations, whereas the remaining 9 were confirmed by follow-up (the follow-up time was from 6 mo to 5 yr after radiotherapy, with a median time of 2.5 yr).

For the 51 patients in the fibrotic group (including 40 men and 11 women), the median age was 46 years (ranging from 21 to 77 yr). Forty-two were confirmed with fibrosis after radiotherapy by pathological examination, whereas the remaining 9 were confirmed by follow-up.

Seventy patients were included in the clivus recurrence and clivus nonrecurrence groups, all of them confirmed by follow-up. The follow-up time was from 6 months to 5 years after radiotherapy, with a median time of 2.5 years. Twenty-two of the patients were in the clivus recurrence group (including 18 men and 4 women); their median age was 49 years (ranging from 26 to 82 yr). For the 48 patients in the clivus nonrecurrence group (including 40 men and 8 women), the median age was 46 years (ranging from 21 to 77 yr).

3.3. Conventional MRI results

Images from 39 recurrent NPC patients showed different degrees of swelling of the nasopharyngeal wall or mass. Recurrent lesions on conventional MRI presented as longer T1 and longer T2 signals, and enhanced MRI presented as moderate enhancement (39/39, 100%) (Fig. 1). Local swelling of the nasopharyngeal wall in the 51 cases of the fibrotic group was not as obvious as in the recurrence group on contrast sequences. Fibrotic lesions on conventional and contrast MRI presented as similar signal to that of the recurrent group (51/51, 100%).

In the clivus recurrence group, 14 patients (14/22, 63.6%) were with nasopharyngeal wall thickening, whereas the other 8 (8/22, 36.4%) were not. The plain scan in all patients showed slightly longer T1 and T2 signals (22/22, 100%). The enhanced scan showed that 9 (9/22, 40.9%) and 5 (5/22, 22.7%) patients were with evident and moderate enhancement, respectively; all these

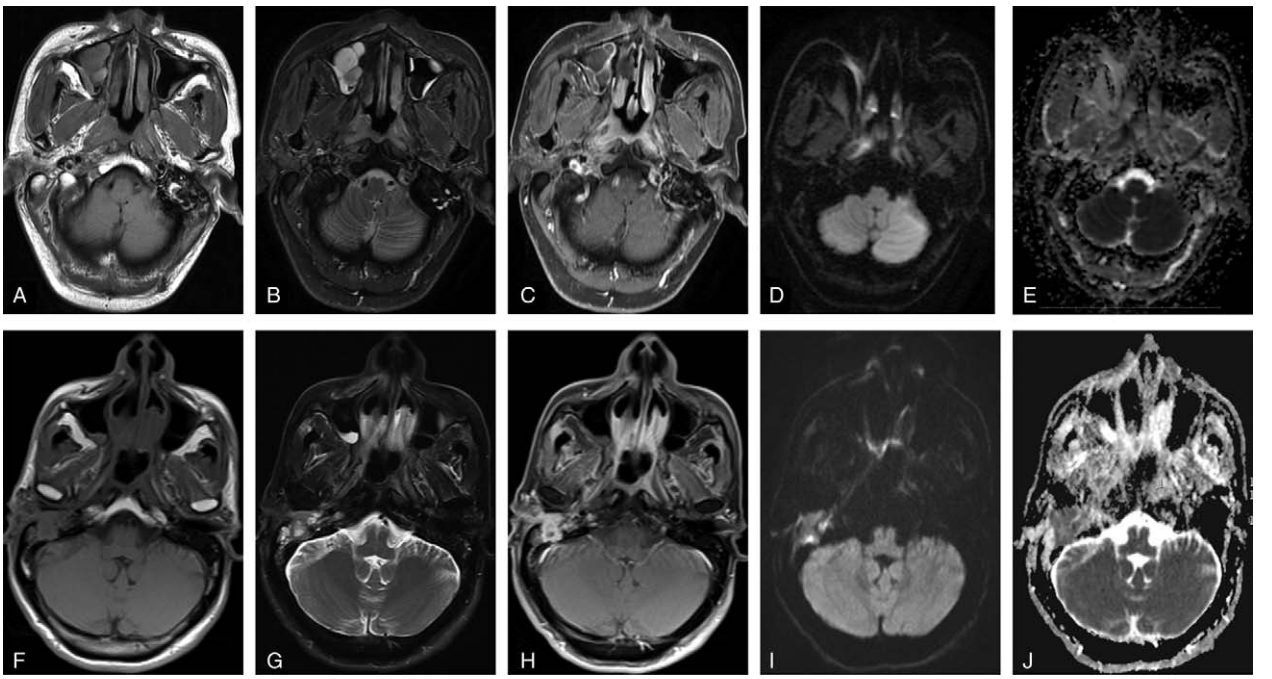

Figure 1. Male, 40 years old. August 23, 2014. Local recurrence of nasopharyngeal carcinoma 2 years after radiotherapy. A, Cross-sectional T1WI plain image showing swollen thick lateral walls and posterior wall of nasopharynx with slight hypointensity. B, Cross-sectional T2WI plain image showing swollen thick lateral walls and posterior wall of nasopharynx with slight hyper-intensity. C, Cross-sectional T1W1 enhanced image showing swollen thick lateral walls and posterior wall of nasopharynx with significant hyperintensity, indicating tumor recurrence. D, diffusion-weighted imaging (DWI) lesions indicating high signal on the right lateral wall. E, The apparent diffusion coefficient (ADC) diagram showing the partially low signal performance on the right side wall. The ADC value of the lesion is 0.882×10^{-3} mm^2/s. Male, 47 years old. December 25, 2015. Localized fibrosis 1 year afterradiotherapy. F, Cross-sectional T1WI plain image showing swollen thick lateral walls of the nasopharynx with slight hypo-intensity. G, Cross-sectional T2WI plain image showing swollen thick lateral walls of the nasopharynx with slight hyper-intensity. H, Cross-sectional T1WI enhanced image showing swollen thick lateral walls of the nasopharynx with significant hyper-intensity that are similar to recurrent lesions. I, DWI lesions with hypo-intensity. J, The ADC diagram shows lesions with hyper-intensity. The ADC value of the lesion is 1.439×10^{-3} mm^2/s. T1WI = T1-weighted imaging, T2WI = T2-weighted imaging.

14 patients were with nasopharyngeal wall thickening. In contrast, 5 (5/22, 22.7%) and 3 (3/22, 13.6%) patients were with mild enhancement and no enhancement, respectively; all these 8 patients were without nasopharyngeal wall thickening (Fig. 2).

For the clivus nonrecurrence group, 23 patients (23/48, 47.9%) were with nasopharyngeal wall thickening, whereas the other 25 (25/48, 52.1%) were not. The plain scan showed slightly longer T1 and T2 signals in 23 patients (23/48, 47.9%). The enhanced scan showed that 6 (6/48, 12.5%) and 17 (17/48, 35.4%) patients were with moderate and evident enhancement, and all of these 23 patients were with nasopharyngeal wall thickening. The remaining 25 patients (25/48, 52.1%) without nasopharyngeal wall thickening were without enhancement (Fig. 3).

For the clivus nonrecurrence group, 44 patients (44/48, 91.7%) were found with high signals on DWI images and iso- or slightly high signals on the ADC images. Four patients (4/48, 8.3%) were with iso- or slightly low signals on the DWI images and iso- or slightly low signals on the ADC images (Fig. 3).

3.4. DWI results

Thirty-nine cases of recurrent NPC showed high or slightly higher signals on DWI and all of them showed low signals on ADC maps (Fig. 1D–E). Fifty-one patients of the fibrotic group showed slightly lower signals than those of the recurrence group on DWI. On ADC maps, 36 cases of the fibrotic group showed equal or slightly low signal performance and the remaining 15 cases showed moderate high signal (Fig. 1I–J).

For the clivus recurrence group, DWI showed high signals in 17 patients (17/22, 77.3%) and isosignals in 4 patients (4/22, 18.2%). The lesions of these 21 patients (21/22, 95.5%) in the ADC images showed low or slightly low signals. The remaining patient (1/22, 4.5%) was with isosignal in the DWI image, and with slightly high signal in the ADC image (Fig. 2).

3.5. Diagnostic performance

The average ADC value in the recurrence group ($0.753 \pm 0.127 \times 10^{-3}$ mm^2/s) was significantly lower than that of the fibrotic group ($1.233 \pm 0.310 \times 10^{-3}$ mm^2/s) ($P < .0001$). The mean ADC values in the clivus recurrence group and clivus nonrecurrence group were $0.780 \pm 0.166 \times 10^{-3}$ and $1.666 \pm 0.342 \times 10^{-3}$ mm^2/s, respectively ($P = .002$).

When the ADC threshold of the recurrence group was 0.887×10^{-3} mm^2/s, the sensitivity, specificity, positive predictive value, negative predictive value, and area under the curve (AUC) of DWI for recurrent NPC were 0.8717, 0.9411, 0.9189, 0.9057, and 0.967, respectively. The sensitivity, specificity, positive predictive value, negative predictive value, and AUC of conventional MRI for recurrent NPC were 0.7179, 0.7451, 0.6829, 0.9268, and 0.732, respectively (Table 2). The area under the ROC curve was significantly different ($P < .001$) between MR DWI and conventional MRI (Fig. 4).

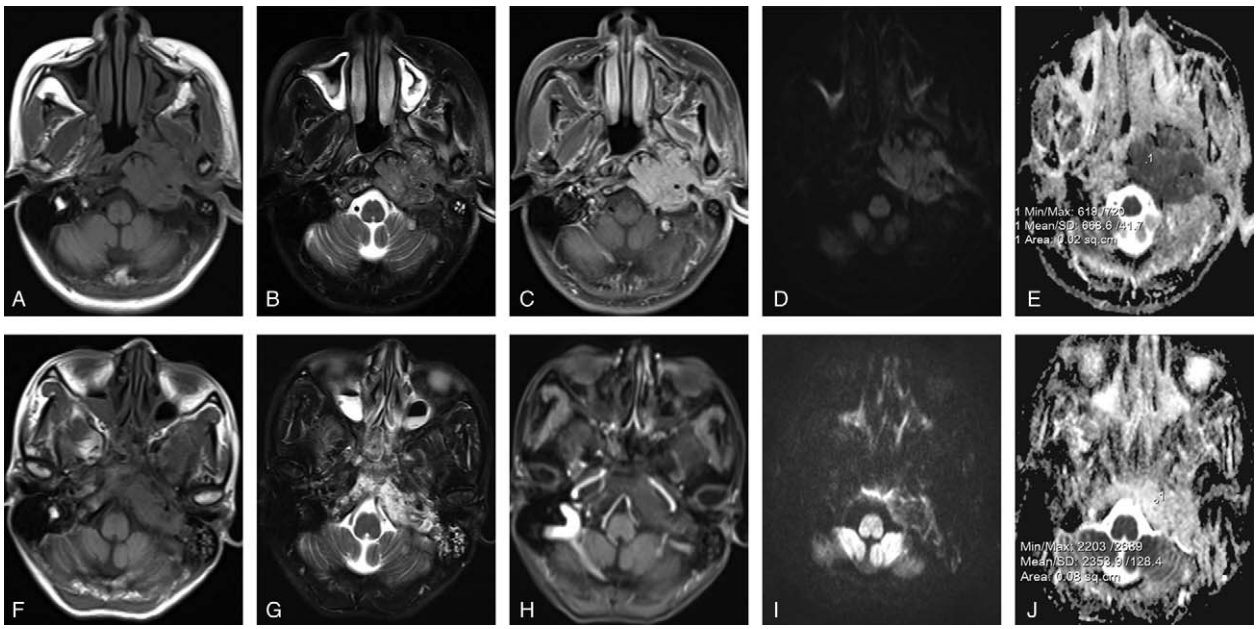

Figure 2. A–E, Female, 42 years old. March 18, 2011. The patient had received treatments for nasopharyngeal carcinoma (NPC) 2 years before, and was highly suspected with clivus recurrent NPC according to imaging and medical history. A, T1WI plain scan. B, T2WI plain scan. C, T1WI enhanced scan. D, Diffusion-weighted imaging (DWI) image showing high signals of the lesion before radiotherapy. E, Apparent diffusion coefficient (ADC) image showing low signals of the lesion before radiotherapy. The ADC value of the lesion area was $0.668 \times 10^{-3} mm^2/s$. All these findings suggest abnormal signals at the clivus of the skull base. F–J, Female, 42 years old. November 11, 2011. F, T1WI plain scan. G, T2WI plain scan. H, T1WI enhanced scan. All these 3 images were obtained after radiotherapy and showed that the range of the abnormal signals decreased after treatment, which confirmed the recurrence of NPC. The patient was followed. I, DWI image after radiotherapy, showing high signals of the lesion. J, ADC image showing low signals of the lesion after radiotherapy. The ADC value in the lesion area was $2.353 \times 10^{-3} mm^2/s$. T1WI = T1-weighted imaging, T2WI = T2-weighted imaging.

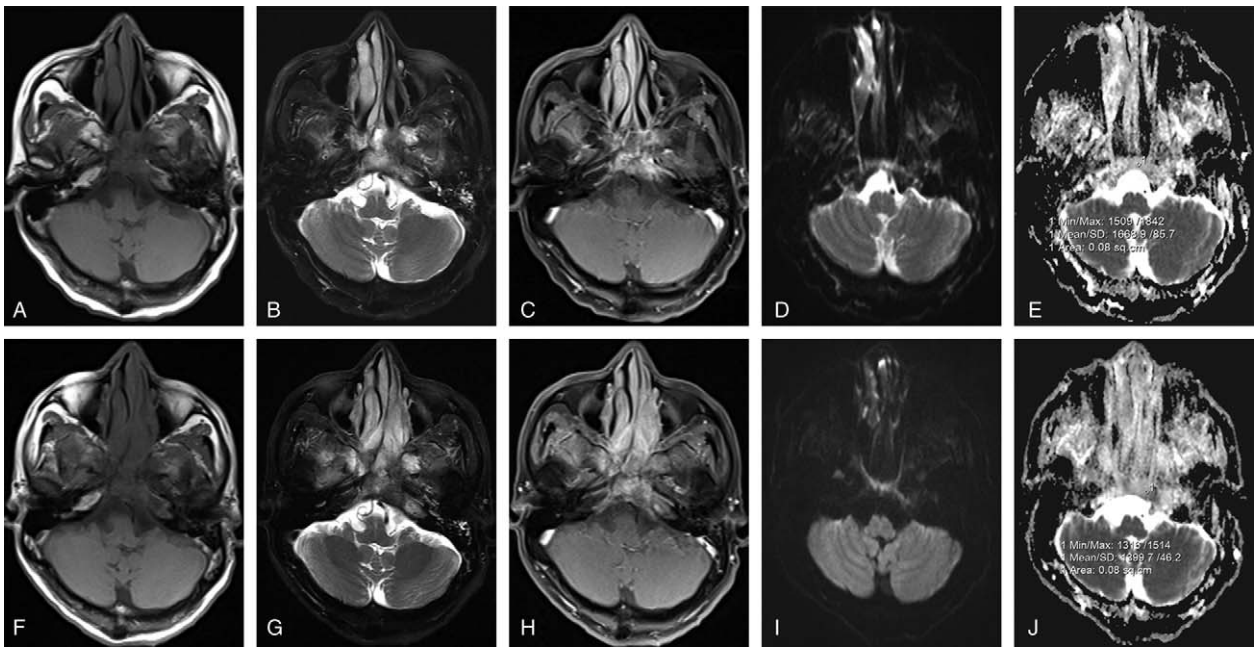

Figure 3. A–E, Male, 56 years old. November 29, 2012. This patient had received treatments for nasopharyngeal carcinoma (NPC) 1 year before, and was highly suspected with postradiotherapy changes in the clivus. A, T1WI plain scan. B, T2WI plain scan. C, T1WI enhanced scan. D, Diffusion-weighted imaging (DWI) image showing high signals of the lesion before follow-up. E, Apparent diffusion coefficient (ADC) image showing high signals of the lesion before follow-up. The ADC value in the lesion area was $1.668 \times 10^{-3} mm^2/s$. F–J, Male, 56 years old. March 11, 2013. The images during follow-up suggested postradiotherapy changes. F, T1WI plain scan. G, T2WI plain scan. H, T1WI enhanced scan. All 3 images were obtained at 3 months of follow-up, and showed that the range of the abnormal signals in the clivus did not change evidently. The patient was further followed after being confirmed with post-radiotherapy changes. I, DWI image of the patient at 3 months of follow-up, showing high signals of the lesion. J, ADC image of the patient at 3 months of follow-up. The ADC value in the lesion area was $1.399 \times 10^{-3} mm^2/s$. T1WI = T1-weighted imaging, T2WI = T2-weighted imaging.

Table 2

Diagnostic performance of recurrent nasopharyngeal carcinoma by routine magnetic resonance imaging and diffusion-weighted imaging.

		Routine MRI		DWI	
Result confirmed by pathology or follow-up	Total	(+)	(−)	(+)	(−)
(+)	39	28	11	34	5
(−)	51	13	38	3	48
	90	41	49	37	53
	Positive predictive value	0.6829		0.9189	
	Negative predictive value	0.9268		0.9057	

The sensitivity and specificity of DWI were 0.8717 and 0.9411, respectively.
The sensitivity and specificity of routine MRI were 0.7179 and 0.7451, respectively.
DWI = diffusion-weighted imaging, MRI = magnetic resonance imaging.

Table 3

Effectiveness of magnetic resonance imaging and diffusion-weighted imaging in diagnosing clivus recurrent nasopharyngeal carcinoma.

		MRI		DWI	
Results confirmed by follow-up	Total	(+)	(−)	(+)	(−)
(+)	22	14	8	21	1
(−)	48	25	23	4	44
	70	39	31	25	45
Positive predictive value		0.3590		0.8400	
Negative predictive value		0.7419		0.9778	

The sensitivity and specificity of DWI were 0.9545 and 0.9167, respectively.
The sensitivity and specificity of MRI were 0.6363 and 0.4791, respectively.
DWI = diffusion-weighted imaging, MRI = magnetic resonance imaging.

Using $<1.018\times10^{-3}\,mm^2/s$ as the threshold of ADC in diagnosing clivus recurrent NPC, the sensitivity, specificity, positive predictive value, negative predictive value, and AUC of DWI for recurrent NPC were 0.9545, 0.9167, 0.8400, 0.9778, and 0.984, respectively (Fig. 4). The sensitivity, specificity, positive predictive value, negative predictive value, and AUC of conventional MRI for skull base recurrent NPC was 0.6363, 0.4791, 0.3590, 0.7419, and 0.558, respectively (Table 3). The AUC of DWI and conventional MRI was significantly different ($P<.001$) (Fig. 5).

4. Discussion

Tumor recurrence is the major cause of treatment failure for NPC. Early identifying the tumor recurrence and provide treatments in time are critical for increasing survival and improve quality of life. The clivus of the skull base is one of the most common sites of NPC recurrence.[17] DWI is used for a variety of cancers, but few data are available for NPC. Therefore, this study aimed to investigate the DWI features of recurrent NPC after radiotherapy, and ADC thresholds for the diagnosis of recurrent NPC. The results showed that DWI has higher diagnostic value for recurrent NPC than MRI. DWI can increase the sensitivity and specificity of diagnosing locally recurrent NPC.

Conventional MRI can display the locations, range, and lymph node metastasis of most NPCs, but it is very difficult for conventional MRI to accurately identify recurrent NPC from fibrosis after radiotherapy, radiation osteomyelitis, or responsive inflammation.[5] The major reason is that the recurrent tumor after NPC radiotherapy and the nonrecurrent lesion both show slightly longer T1 and T2 signals in conventional MRI, and show different enhancement in enhanced scanning.[12,15,18] Therefore, using conventional MRI makes very difficult to clearly diagnose early recurrent tumors and multiple follow-ups are needed to observe the changes of the nasopharyngeal cavity. The present study showed that the sensitivity and specificity of conventional MRI in diagnosing local and clivus recurrent NPC were both relatively low (71.79% and 74.51% for locally recurrent NPC,

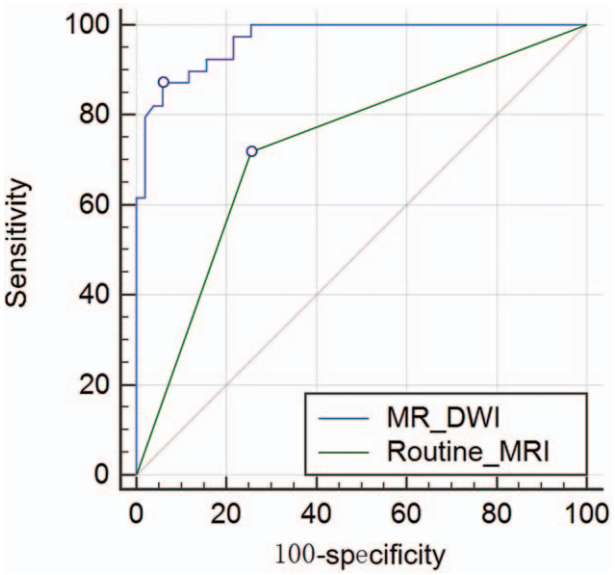

Figure 4. Receiver operating characteristics (ROC) curve of DWI in diagnosing local recurrent nasopharyngeal carcinoma (NPC). DWI = diffusion-weighted imaging, MRI = magnetic resonance imaging.

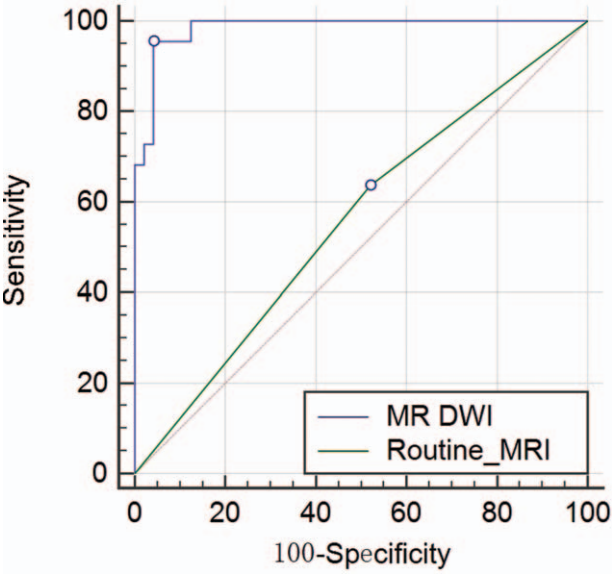

Figure 5. Receiver operating characteristics (ROC) curve of MR DWI in diagnosing clivus recurrent nasopharyngeal carcinoma (NPC). MR DWI = magnetic resonance diffusion-weighted imaging.

and 63.63% and 47.91% for clivus recurrent NPC). Based on previous studies,[19,20] it may be hypothesized that the similarities between recurrent tumor and nonrecurrent tumor lesions on conventional MRI are associated with pathological changes such as congestion, edema, and inflammation in the local soft tissue of the NPC area after radiotherapy, and these changes can last for several months to several years. These changes are in fact the major causes of the difficulties in identifying locally recurrent tumors from nonrecurrent lesions on conventional MRI images after radiotherapy of NPC.

DWI is a noninvasive imaging technique that can be used to observe the free diffusion of water molecules at the molecular level in living organisms. This technique can detect early pathological changes related with the changes of water volume in tissues.[18,21] Previous studies have shown that ADC values of tumors are positively associated with the differentiation of tumor cells.[10,12–16,22,23] DWI has already been applied in the diagnosis of prostate, breast, and liver diseases.[19,20] Previous studies about the diagnosis of NPC demonstrated that compared with conventional MRI, DWI could detect distant metastases of NPC and postradiotherapy biological changes earlier, and with higher sensitivity and specificity,[10,24] as observed in the present study. This method could compensate the limitations of conventional imaging diagnosis and provide additional, more accurate evidence for clinical staging, assessing biological behaviors of the tumors, evaluating treatment efficacy, and assessing prognosis. The present study also showed that the ADC values of the primary NPC and lesions with muscle involvement were lower than normal tissues, which showed high and low signals in the DWI and ADC images, respectively. These findings are in agreement with previous findings.[25,26] In addition, the present study also showed that the ADC values of recurrent NPC were significantly lower than that of the nonrecurrent lesions. Furthermore, the present study also demonstrated that DWI has relatively high diagnostic power for recurrent tumor compared with conventional MRI. Nevertheless, DWI often shows more artifacts than conventional MRI sequences and there is thus a probability of missing small lesions.[27,28] Additional studies with the combination of different and multiple *b* values could overcome this issue, as suggested in prostate cancer.[29]

The mechanism underlying the association between a high pretreatment ADC value and local failure may be correlated with the radiosensitivity of the tumor.[21,30,31] Indeed, a number of biological features such as hypoxia, inflammation, cell density, and cell membrane integrity affect the diffusion of water in tissues and hence the ADC value, and these factors may also influence the radiosensitivity of the tumor. For example, tumor hypoxia promotes inflammation, which is correlated with a high ADC value as it increases the interstitial water content of the tissue,[32,33] and hypoxia is a well-known characteristic associated with low radiosensitivity.[34,35] On the contrary, ADC values are inversely correlated with cell density in many malignancies, and tumors with a high cell density are more likely to have a higher number of viable proliferative cells and may exhibit a better response to radiotherapy.[36,37] Therefore, it is expected that tumors with fewer viable proliferative cells would have high ADC values and lower radiosensitivity. Nevertheless, these mechanisms still need to be confirmed in NPC.

It has to be noted that the diagnostic thresholds of the recurrent tumor at the nasopharynx and clivus of skull base were different. The diagnostic threshold of the recurrent tumor at the clivus of skull base was higher than nasopharynx. When using 1.018×10^{-3} mm^2/s as the diagnostic threshold for recurrent tumor at the clivus, the sensitivity and specificity were both the highest, and the lesions at the clivus all showed relatively higher signals on the ADC images than normal bone marrow. Based on a previous study[38] and the analysis of the age of the patients in the present study, we speculated that this finding could be associated with the fact that all the patients in the present study were adults with a large amount of adipose tissue in the clivus, and the imaging sequence used by the DWI has adipose-pressing effects.

This study has several limitations. First, the number of patients was relatively small. Secondly, the variation of ADC values in the nonrecurrent group was relatively high, which could be associated with the differences in the evolution of the pathological changes of the tissues in the nonrecurrent group. Thirdly, the data about the optimization of the multi-*b* values in the DWI sequences were unavailable. Fourthly, only highly suspicious cases during clinical and MRI follow-up were examined by nasopharyngoscopy; not all patients within 6 months after radiotherapy were confirmed by biopsy, but by PET/CT and clinical follow-up. Fifthly, the anatomical structure of the skull base is complex. Thus, susceptibility artifacts or image drift often occurs on DWI images, although preventive measures were taken including placing a padded oil pillow below the neck of the patients when scanning, and determining the ROI based on the location of the spinal cord in fused images. Finally, the follow-up period was short. Further studies with larger sample sizes and more specific investigations are needed to confirm our findings.

In conclusion, DWI has higher diagnostic value than conventional MRI for diagnosing recurrent NPC. The diagnostic power was the highest when using 0.887×10^{-3} and 1.018×10^{-3} mm^2/s as the threshold for diagnosing local and clivus recurrent NPC, respectively. Because DWI is very easy to operate, we recommend to use this technology as a routine imaging modality for patients with NPC.

Author contributions

Conceptualization: Lidong Liu, Shaolv Lai, Danke Su, Ningbin Luo.
Data curation: Shaolv Lai, Younan Liu.
Formal analysis: Shaolv Lai, Guanqiao Jin.
Funding acquisition: Chen Wang, Younan Liu.
Investigation: Lidong Liu, Shaolv Lai, Younan Liu.
Methodology: Guanqiao Jin, Xuna Zhu.
Project administration: Chen Wang, Shaolv Lai, Guanqiao Jin.
Software: Chen Wang, Lidong Liu, Shaolv Lai, Danke Su, Xuna Zhu.
Supervision: Xuna Zhu, Ningbin Luo.
Validation: Chen Wang, Danke Su, Younan Liu.
Visualization: Lidong Liu, Ningbin Luo.
Writing – original draft: Chen Wang, Lidong Liu, Guanqiao Jin, Ningbin Luo.
Writing – review and editing: Chen Wang, Lidong Liu, Guanqiao Jin, Ningbin Luo.

References

[1] Zhou Q, He Y, Zhao Y, et al. A study of 358 cases of locally advanced nasopharyngeal carcinoma receiving intensity-modulated radiation therapy: improving the seventh edition of the American Joint Committee on Cancer T-Staging System. Biomed Res Int 2017;2017:1419676.
[2] Mao J, Shen J, Yang Q, et al. Intravoxel incoherent motion MRI in differentiation between recurrent carcinoma and postchemoradiation fibrosis of the skull base in patients with nasopharyngeal carcinoma. J Magn Reson Imaging 2016;44:1556–64.

[3] Yang TS, Ng KT, Wang HM, et al. Prognostic factors of locoregionally recurrent nasopharyngeal carcinoma—a retrospective review of 182 cases. Am J Clin Oncol 1996;19:337–43.
[4] Han J, Zhang Q, Kong F, et al. The incidence of invasion and metastasis of nasopharyngeal carcinoma at different anatomic sites in the skull base. Anat Rec (Hoboken) 2012;295:1252–9.
[5] Altun M, Tenekeci N, Kaytan E, et al. Locally advanced nasopharyngeal carcinoma: computed tomography findings, clinical evaluation, and treatment outcome. Int J Radiat Oncol Biol Phys 2000;47:401–4.
[6] Wei WI, Sham JS. Nasopharyngeal carcinoma. Lancet 2005;365: 2041–54.
[7] Mohandas A, Marcus C, Kang H, et al. FDG PET/CT in the management of nasopharyngeal carcinoma. AJR Am J Roentgenol 2014;203:W146–57.
[8] Zhou H, Shen G, Zhang W, et al. 18F-FDG PET/CT for the diagnosis of residual or recurrent nasopharyngeal carcinoma after radiotherapy: a metaanalysis. J Nucl Med 2016;57:342–7.
[9] Ng SH, Chan SC, Yen TC, et al. Staging of untreated nasopharyngeal carcinoma with PET/CT: comparison with conventional imaging work-up. Eur J Nucl Med Mol Imaging 2009;36:12–22.
[10] Jin G, Su DK, Luo NB, et al. Meta-analysis of diffusion-weighted magnetic resonance imaging in detecting prostate cancer. J Comput Assist Tomogr 2013;37:195–202.
[11] Hong J, Yao Y, Zhang Y, et al. Value of magnetic resonance diffusion-weighted imaging for the prediction of radiosensitivity in nasopharyngeal carcinoma. Otolaryngol Head Neck Surg 2013;149:707–13.
[12] Hatakenaka M, Nakamura K, Yabuuchi H, et al. Pretreatment apparent diffusion coefficient of the primary lesion correlates with local failure in head-and-neck cancer treated with chemoradiotherapy or radiotherapy. Int J Radiat Oncol Biol Phys 2011;81:339–45.
[13] King AD, Chow KK, Yu KH, et al. Head and neck squamous cell carcinoma: diagnostic performance of diffusion-weighted MR imaging for the prediction of treatment response. Radiology 2013;266:531–8.
[14] Luo N, Su D, Jin G, et al. Apparent diffusion coefficient ratio between axillary lymph node with primary tumor to detect nodal metastasis in breast cancer patients. J Magn Reson Imaging 2013;38:824–8.
[15] Lambrecht M, Van Calster B, Vandecaveye V, et al. Integrating pretreatment diffusion weighted MRI into a multivariable prognostic model for head and neck squamous cell carcinoma. Radiother Oncol 2014;110:429–34.
[16] Ohnishi K, Shioyama Y, Hatakenaka M, et al. Prediction of local failures with a combination of pretreatment tumor volume and apparent diffusion coefficient in patients treated with definitive radiotherapy for hypopharyngeal or oropharyngeal squamous cell carcinoma. J Radiat Res 2011;52:522–30.
[17] Yi W, Liu ZG, Li X, et al. CT-diagnosed severe skull base bone destruction predicts distant bone metastasis in early N-stage nasopharyngeal carcinoma. Onco Targets Ther 2016;9:7011–7.
[18] Xu JF, Wu XW, Wang WQ, et al. Value of diffusion-weighted magnetic resonance imaging on the follow-up of nasopharyngeal carcinoma after radiotherapy. J Xray Sci Technol 2014;22:605–12.
[19] Panebianco V, Sciarra A, Marcantonio A, et al. Conventional imaging and multiparametric magnetic resonance (MRI, MRS, DWI, MRP) in the diagnosis of prostate cancer. Q J Nucl Med Mol Imaging 2012;56:331–42.
[20] Uwano I, Sasaki M, Kudo K, et al. Diffusion anisotropy color-coded map of cerebral white matter: quantitative comparison between orthogonal anisotropic diffusion-weighted imaging and diffusion tensor imaging. J Neuroimaging 2013;23:197–201.
[21] Zhang Y, Liu X, Zhang Y, et al. Prognostic value of the primary lesion apparent diffusion coefficient (ADC) in nasopharyngeal carcinoma: a retrospective study of 541 cases. Sci Rep 2015;5:12242.
[22] Asao C, Korogi Y, Kitajima M, et al. Diffusion-weighted imaging of radiation-induced brain injury for differentiation from tumor recurrence. AJNR Am J Neuroradiol 2005;26:1455–60.
[23] Roquer J, Rodriguez-Campello A, Cuadrado-Godia E, et al. Acute brain MRI-DWI patterns and stroke recurrence after mild-moderate stroke. J Neurol 2010;257:947–53.
[24] Eiber M, Holzapfel K, Ganter C, et al. Whole-body MRI including diffusion-weighted imaging (DWI) for patients with recurring prostate cancer: technical feasibility and assessment of lesion conspicuity in DWI. J Magn Reson Imaging 2011;33:1160–70.
[25] Genovesi D, Filippone A, Ausili Cefaro G, et al. Diffusion-weighted magnetic resonance for prediction of response after neoadjuvant chemoradiation therapy for locally advanced rectal cancer: preliminary results of a monoinstitutional prospective study. Eur J Surg Oncol 2013;39:1071–8.
[26] Cieszanowski A, Anysz-Grodzicka A, Szeszkowski W, et al. Characterization of focal liver lesions using quantitative techniques: comparison of apparent diffusion coefficient values and T2 relaxation times. Eur Radiol 2012;22:2514–24.
[27] Osman NM, Rahman AA, Ali MT. The accuracy and sensitivity of diffusion-weighted magnetic resonance imaging with apparent diffusion coefficients in diagnosis of recurrent cholesteatoma. Eur J Radiol Open 2017;4:27–39.
[28] Schwartz KM, Lane JI, Bolster BDJr, et al. The utility of diffusion-weighted imaging for cholesteatoma evaluation. AJNR Am J Neuroradiol 2011;32:430–6.
[29] Ning P, Shi D, Sonn GA, et al. The impact of computed high b-value images on the diagnostic accuracy of DWI for prostate cancer: a receiver operating characteristics analysis. Sci Rep 2018;8:3409.
[30] Ni X, Tong Y, Xiao Y, et al. Diffusion-weighted magnetic resonance imaging in predicting the radiosensitivity of cervical cancer. Int J Clin Exp Med 2015;8:13836–41.
[31] Larocque MP, Syme A, Allalunis-Turner J, et al. ADC response to radiation therapy correlates with induced changes in radiosensitivity. Med Phys 2010;37:3855–61.
[32] Hompland T, Ellingsen C, Galappathi K, et al. DW-MRI in assessment of the hypoxic fraction, interstitial fluid pressure, and metastatic propensity of melanoma xenografts. BMC Cancer 2014;14:92.
[33] Huang Z, Xu X, Meng X, et al. Correlations between ADC values and molecular markers of Ki-67 and HIF-1alpha in hepatocellular carcinoma. Eur J Radiol 2015;84:2464–9.
[34] Kato Y, Yashiro M, Fuyuhiro Y, et al. Effects of acute and chronic hypoxia on the radiosensitivity of gastric and esophageal cancer cells. Anticancer Res 2011;31:3369–75.
[35] Rockwell S, Dobrucki IT, Kim EY, et al. Hypoxia and radiation therapy: past history, ongoing research, and future promise. Curr Mol Med 2009;9:442–58.
[36] Gibbs P, Liney GP, Pickles MD, et al. Correlation of ADC and T2 measurements with cell density in prostate cancer at 3.0 Tesla. Invest Radiol 2009;44:572–6.
[37] Chen L, Liu M, Bao J, et al. The correlation between apparent diffusion coefficient and tumor cellularity in patients: a meta-analysis. PLoS One 2013;8:e79008.
[38] Ginat DT, Mangla R, Yeaney G, et al. Diffusion-weighted imaging for differentiating benign from malignant skull lesions and correlation with cell density. AJR Am J Roentgenol 2012;198:W597–601.